

496950

GRANT  
IN-39-CR

153098

P 11

NAG1-1329

**Hypervelocity Impact Study Interim Report:  
The Effect of Impact Angle on Crater Morphology**

by

Gary Crawford, Dr. David Hill, Dr. Frank Rose, Dr. Ralph Zee,  
Steve Best, and Mike Crumpler

**Space Power Institute and Materials Engineering  
Auburn University**

March 15, 1993

(NASA-CR-192711) HYPERVELOCITY  
IMPACT STUDY: THE EFFECT OF IMPACT  
ANGLE ON CRATER MORPHOLOGY Interim  
Report (Auburn Univ.) 11 p

N93-25260

Unclas

G3/39 0153098

## **Hypervelocity Impact Study Interim Report: The Effect of Impact Angle on Crater Morphology**

by Gary Crawford, Dr. David Hill, Dr. Frank Rose, Dr. Ralph Zee,  
Steve Best & Mike Crumpler

### **Summary**

The Space Power Institute (SPI) of Auburn University has conducted preliminary tests on the effects of impact angle on crater morphology for hypervelocity impacts. Copper target plates were set at angles of 30° and 60° from the particle flight path. For the 30° impact, the craters looked almost identical to earlier normal incidence impacts. The only difference found was in the apparent distribution of particle residue within the crater, and further research is needed to verify this. The 60° impacts showed marked differences in crater symmetry, crater lip shape, and particle residue distribution. Further research on angle effects is planned, because the particle velocities for these shots were relatively slow (7 km.s<sup>-1</sup> or less).

### **Introduction**

The retrieval of satellites from earth orbit, such as LDEF, has sparked new interest in micrometeorite research. One of the aspects of this research is how impact angle affects the crater morphology of hypervelocity particles. The term 'hypervelocity' is used to describe particles moving faster than 3 to 5 km.s<sup>-1</sup>. This information about impact angle is important because by modeling the phenomena in the laboratory, more information about the micrometeorite flux rate can be determined. This information will aid in future satellite design.

### **Experimental Procedure**

The Hypervelocity Impact Facility (HIF) at SPI was used for these experiments, with two shots having been made thus far. In the first shot, the target plate was set at an angle of 30° with the particle flight path. The angle was 60° in the second shot. (Note: using the nomenclature at HIF, a "0° impact" is one in which the particle's velocity vector is perpendicular to the surface of the target plate. A "90° impact" would have the surface of the plate parallel to the particle flight path.)

Olivine particles of 50 to 100 micrometers in diameter (microgram size) were fired at copper target plates. Olivine was chosen because it simulates natural micrometeorites (composed of silicon, magnesium, and iron), and copper plates were used in order to compare the craters with previous research. Over the past 6 to 8 months, the HIF has been conducting research on the crater morphology and residual debris indicative of olivine impacts on copper plates. A thin mylar film (0.5 μm) was placed over the target plates, such that the mylar was always at a 0° impact angle. The hypervelocity particles pass through the mylar before striking the plate. The mylar allows the particle size to be found, and it helps to prevent gun debris contaminating the surface of the target plate.

The performance of the HIF for these tests was mixed. At the time of the firings, the HIF was set up to fire a limited number of particles. When a small number of

particles are fired, the velocity data for each particle is more reliable. However, if there are less particles, then the likelihood of getting faster particles diminishes. If a large number of particles are fired, there is a greater chance of producing faster particles. Unfortunately, it is harder to ascertain the velocity of the particles that cause a particular crater.

The decision for which technique to use depends on the demands of the researcher. For these tests, we chose a small number of particles because we were unsure of how well the velocity data could be correlated to the impact. The HIF finds the velocity of the impacting particles by measuring the time of impact for a particular crater across the flight path distance. A streak camera 'looks' across the surface of the target plate, and the time of impact is registered by the bright plume of ejecta that comes from the impact site during the crater formation process. For a normal  $0^\circ$  impact, the ejecta plume is basically symmetrical and the location of the crater is easy to find (in fact, the brightness and duration of the plume provides further crater information). But for the  $30^\circ$  and  $60^\circ$  impacts, we were unsure of the plume symmetry. Therefore a smaller number of particles were used in order to better correlate the velocity information.

## Data Analysis

For the analysis of the craters, a Jeol 840 scanning electron microscope with an energy dispersive x-ray system was used. Figure 1 (see the next page) shows the nomenclature used at HIF for describing crater orientation. The side of the crater from which the particle arrives is the leading edge, and the opposite side to this is the trailing edge.

### 30° Impacts

Micrograph 1 shows a typical crater caused by an olivine particle. The particle was traveling 7.0 km/sec, and the crater shape is fairly typical of all the craters analyzed. At first glance, the crater is practically indistinguishable from the  $0^\circ$  impacts of previous shots. The crater is roughly hemispherical, with a diameter to depth ratio of 2.3. The crater lip has no characteristics which hint at the direction of tilt of the plate. The arrow at the bottom left-hand corner of the micrograph shows the direction of the component of the impact velocity vector in the plane of the target. The entire interior of the crater is covered in olivine residue, and the granules inside the crater are 'chunks' of olivine. Upon closer inspection of the interior, there appears to be more olivine residue on the trailing edge interior surface of the crater than on the leading edge of the crater. This phenomena was found in all the olivine craters. However, this analysis is based on morphological considerations, and is tentative at present.

There were several other unusual examples where the crater morphology still conformed to the characteristics in micrograph 1. Sometimes a hypervelocity particle breaks up when it passes through the mylar film, resulting in several closely spaced craters of varying sizes. Micrograph 2 is such a particle. Note how the lips on all the craters give no evidence of plate and particle orientation. These craters were formed by an olivine particle traveling 8.3 km/sec.

When the gun at the HIF launches the particles, a certain amount of debris is carried along with the desired particles. The gun debris is usually of very odd shapes, and any correlation between particle size and crater shape is very hard to attain. Micrograph 3 shows a odd-shaped crater formed by gun debris. Once again, there is nothing in the lip symmetry that provides information about the particle's direction of impact. Micrographs 2 and 3 confirm the phenomena witnessed in micrograph 1.

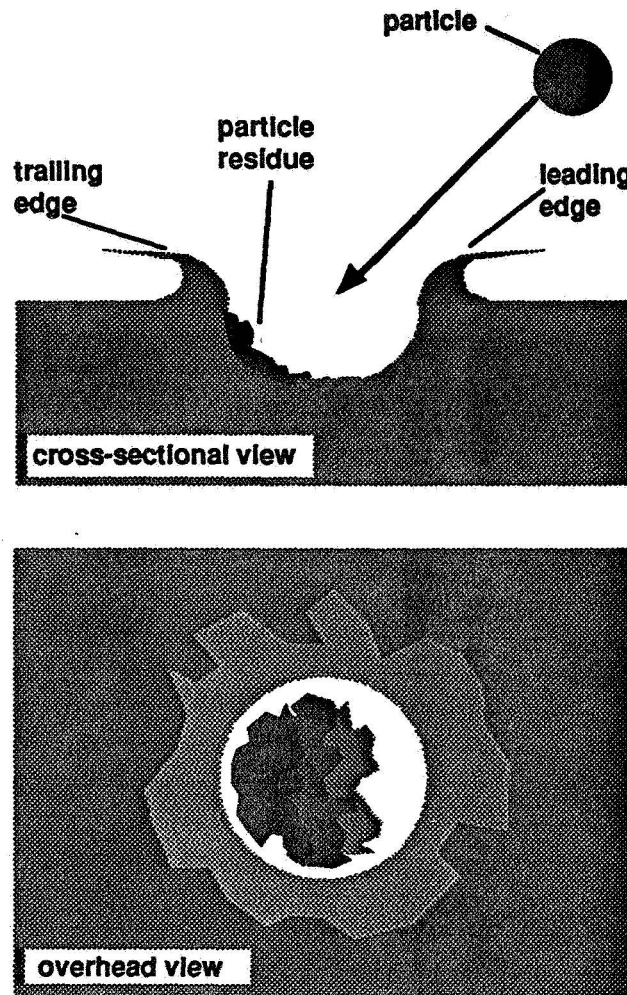


**Figure 1.** Nomenclature used at the Space Power Institute Hypervelocity Impact Facility (HIF) for describing crater orientation. The top diagram shows a cross-sectional view of a crater impacted at some angle. The dark areas inside the crater are particle residue. The darker particle residue signifies higher concentrations, and the lighter color signifies lower residue concentrations. The lower diagram shows an overhead view of the same crater. The crater represented here has the morphological characteristics of a 30° impact.

### 60° Impacts

There was a marked difference between the 60° impacts and the other impacts. The main characteristics, shown in figure 2, were as follows:

1. There was practically no crater lip on the crater leading edge. An extensive lip was found on the crater trailing edge.
2. A great deal more particle residue was found on the trailing interior surface.
3. The crater rims were more elliptical rather than circular in shape.

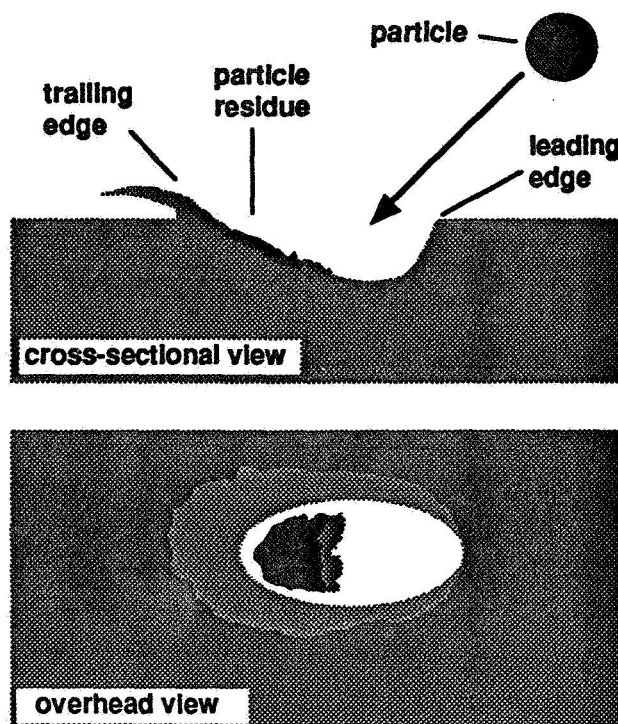


**Figure 2.** *Diagrams of a 60° impact, corresponding to the impact crater shown in Micrograph 4. In the top diagram, there is an extended crater lip on the trailing edge, and no crater lip on the leading edge. The darker particle residue represents the highest concentrations. The lower diagram shows the elliptical crater shape, and the morphology of the lip.*

Micrograph 4 shows one of the 60° impact craters. This crater was formed by an olivine particle traveling 5.6 km/sec. Note the similarity between this Micrograph and Figure 2. The following three micrographs are all of this crater at higher magnification, so that the various features are more obvious.

Micrograph 5 is a close-up of the leading edge. Note how the crater lip gets smaller as the leading edge is approached, until it is practically non-existent at the leading edge (close to the scale bar). This crater has a coating of olivine throughout the crater interior surface, and a few grains of olivine can be seen. This region is also the deepest area in the crater, with a depth of 14  $\mu\text{m}$ . The depth-to-diameter ratio along the minor axis is 0.30, and it is 0.18 along the major axis. Micrograph 6 is of the trailing edge of the crater shown in micrograph 4. There are more olivine grains located here.

Micrograph 7 shows a very interesting phenomena seen on some of the 60° impact craters. Just beyond the crater lip on the trailing edge of the crater, these 'indentations' are found. Some contain small amounts of olivine, and some do not.

As with the other shots, there was some particle breakup. Micrograph 8 shows a 60° impact crater formed by a particle that was fractured. The crater appeared to remain largely intact, because there were few surrounding craters, and this crater was by far the largest. The crater has the same lip symmetry and residue distribution as micrograph 4, although it's rim is more circular than elliptical. The crater is 43  $\mu\text{m}$  deep, and has a

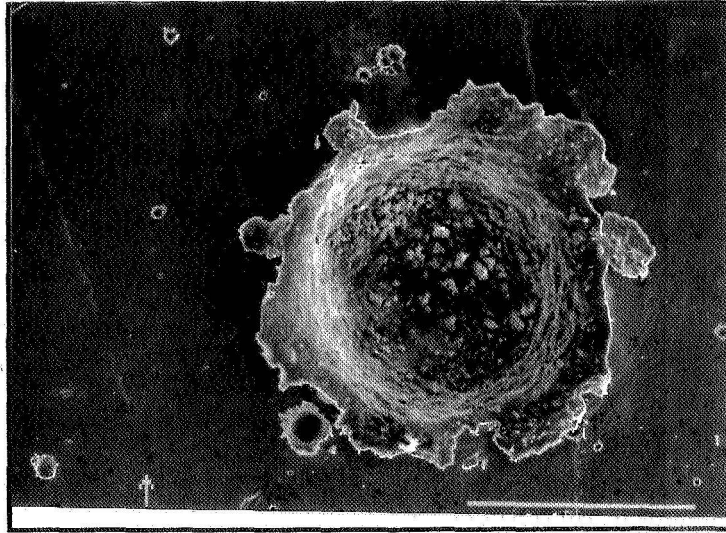
diameter to depth ratio of 3.6. Note that the depth-to-diameter ratio for olivine particles striking a copper plate for a  $0^\circ$  impact is between 0.5 and 0.38. The lighter, 'glowing' material along the interior trailing edge is olivine residue.

Micrograph 9 is of a  $60^\circ$  impact crater formed by gun debris. Even though this is an oddly-shaped crater, it *still* has the characteristic elongation, lip formation, and residual particle debris seen in the previous micrographs. Micrograph 10 is a close-up of the trailing edge of the crater, with the same orientation as micrograph 9. To the left of the trailing edge crater lip, along the interior trailing edge wall, can be seen residual particle material. It is a white, glowing 'clump' of material. There is more particle material in the upper left hand corner. One of the characteristics of the gun debris impacts is a general lack of particle residue, which is only found along the outer edge of the crater lips.

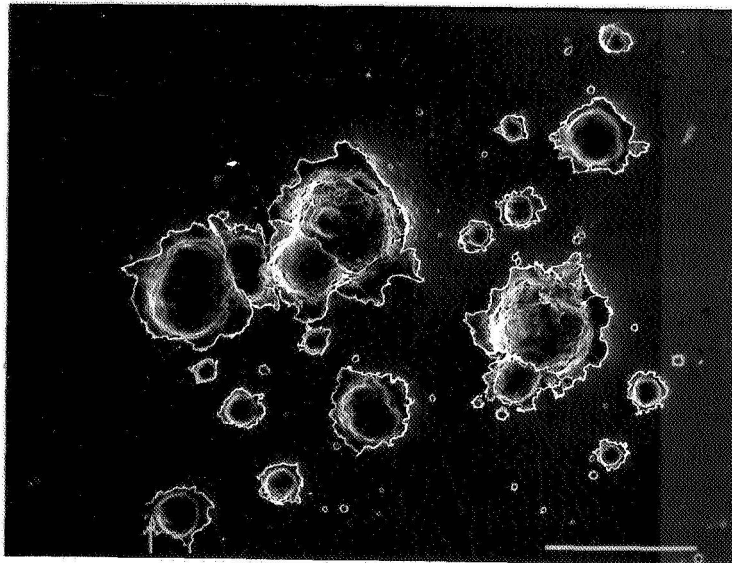
## Conclusion

This preliminary investigation has already seen notable similarities and differences between low and high angle impacts. Both have particle residue distributions different from normal incidence impacts (although it is less pronounced in the lower angle impacts). While the  $30^\circ$  impact craters were still very similar to  $0^\circ$  impacts, the  $60^\circ$  impacts differed substantially. The  $60^\circ$  impacts showed an elliptical crater footprint shape and a crater lip asymmetry between the crater leading edge and trailing edge, with the lip being larger on the trailing edge and almost non-existent on the leading edge.

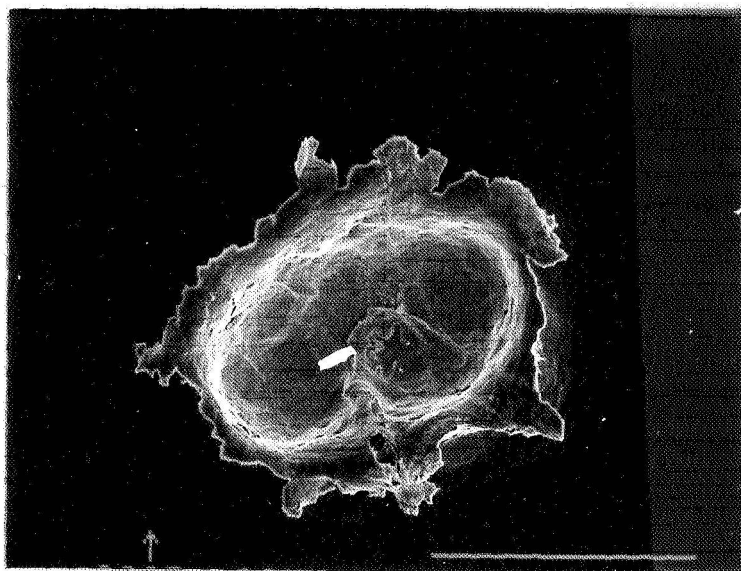
The HIF is currently working on raising particle velocities to previous levels (up to and above  $10 \text{ km.s}^{-1}$ ). Once this has been attained, another  $60^\circ$  shot will be made. Although much useful information has already been acquired, an investment in continued research could provide a wealth of information. More useful information could be provided by making several shots at angles of  $15^\circ$ ,  $30^\circ$ ,  $45^\circ$ ,  $60^\circ$ , and  $75^\circ$ , and using metallographic techniques to measure residual debris in the craters. This could provide extremely valuable information about how the impacting particle's composition is changed by the cratering process. This would aid significantly in investigations which use particle residue from micrometeorites to ascertain the elemental composition of the solar system.



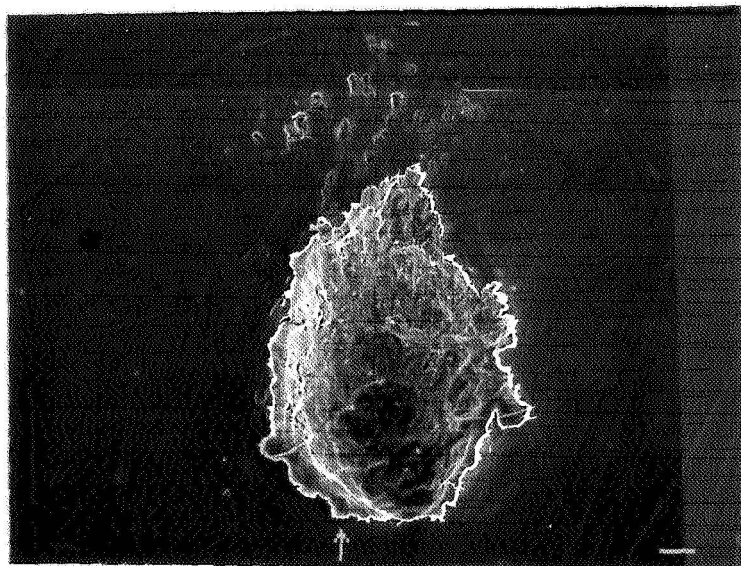
**Micrograph 1:** 30° impact crater formed by olivine particle. Olivine coating throughout the interior, with visible particle grains. Arrow in lower left-hand corner of all micrographs points toward the crater trailing edge. [X300, 100  $\mu\text{m}$  bar,  $V = 7.0 \text{ km.s}^{-1}$ ]



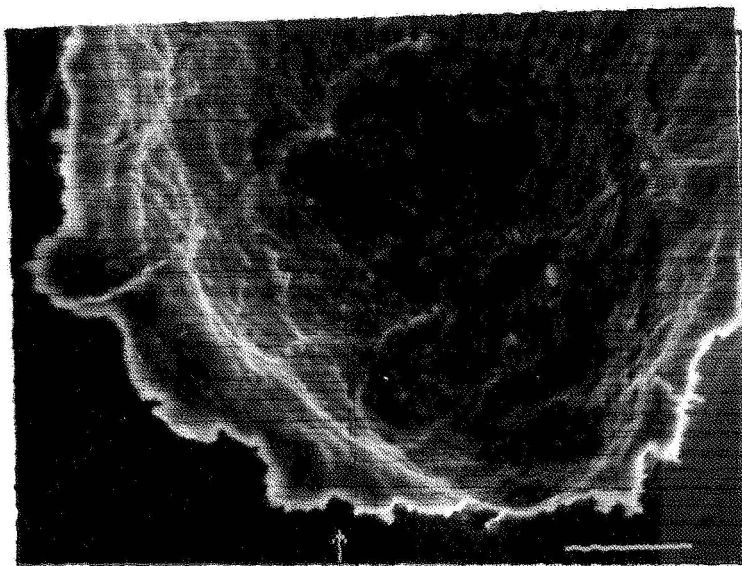
**Micrograph 2:** 30° impact formed by olivine particle which broke up. Note how the morphology is the same as micrograph 1. [X200, 100  $\mu\text{m}$  bar,  $V = 8.3 \text{ km.s}^{-1}$ ].



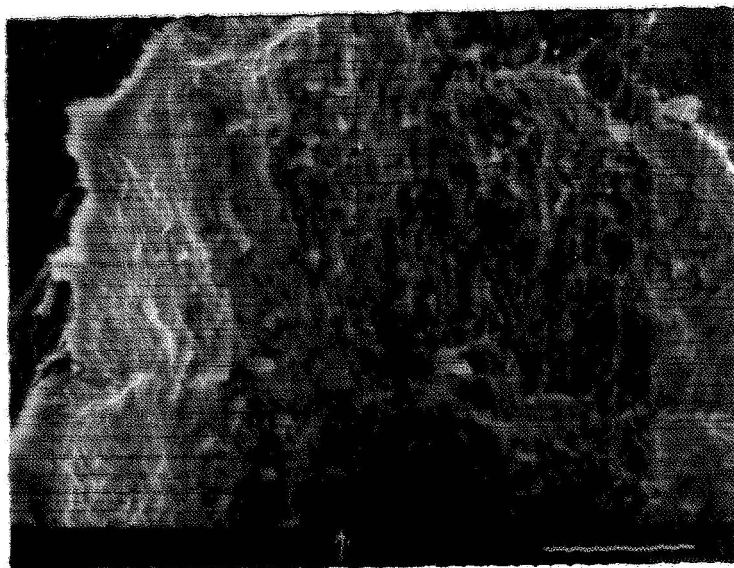
*Micrograph 3: 30° impact formed by gun debris. Note lip symmetry. [ X350, 100  $\mu\text{m}$  bar,  $V = 9.0 \text{ km.s}^{-1}$ ]. Note that the white mark within the crater is an artifact of the photographic development process.*



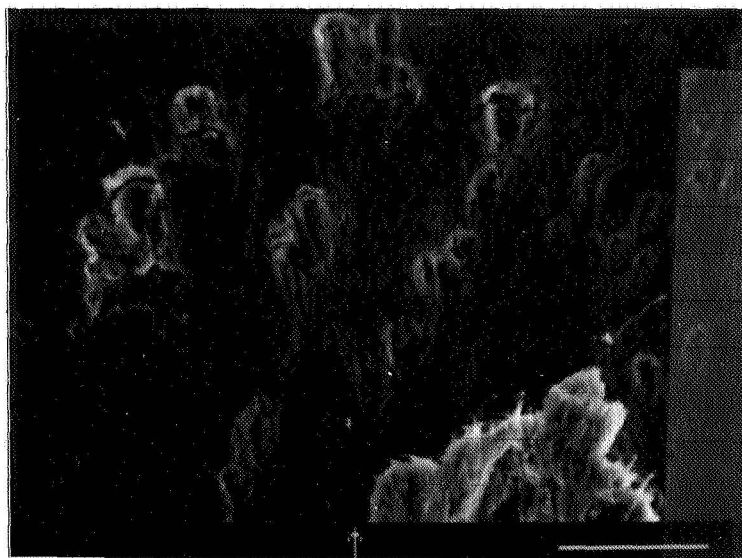
*Micrograph 4: 60° impact formed by olivine. Note elliptical shape of crater. [ X500, 10  $\mu\text{m}$  bar,  $V = 5.6 \text{ km.s}^{-1}$ ]*



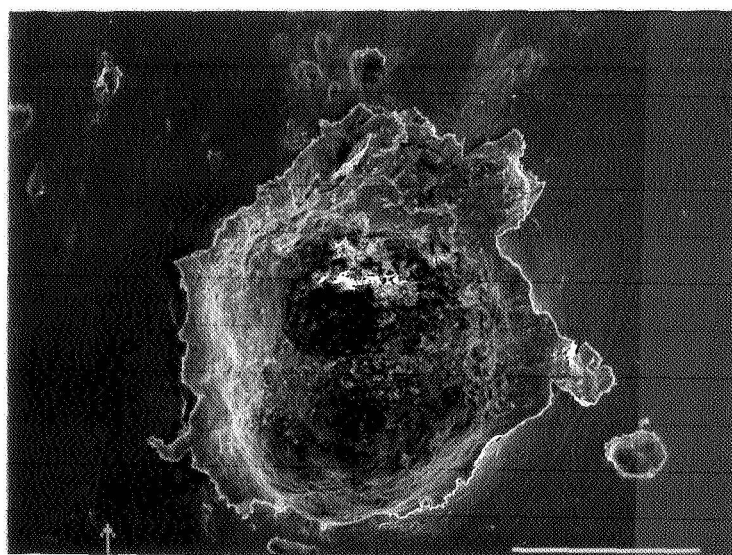
*Micrograph 5: View of micrograph 4 at the leading edge. Note the lack of any crater lip (near the scale bar). [ X1700, 10  $\mu\text{m}$  bar, Vel.= 5.6 km.s<sup>-1</sup>]*



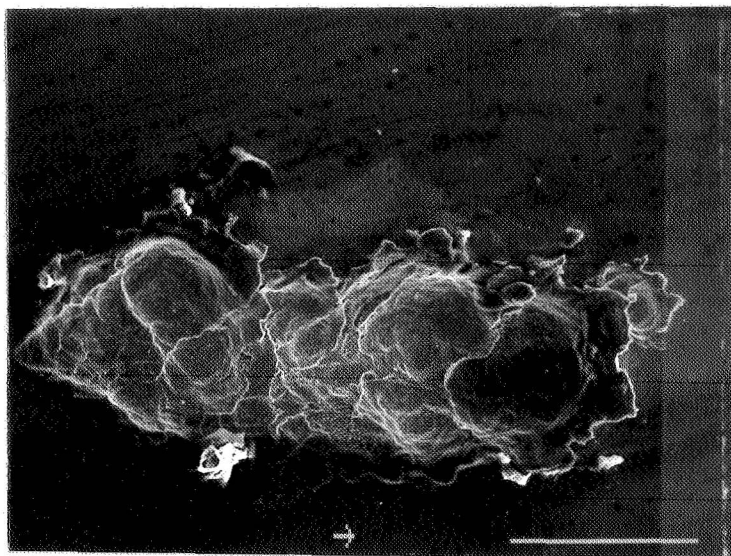
*Micrograph 6: Trailing edge of crater in micrograph 4. Closer inspection shows more olivine grains, and X-ray analysis gives more intense peaks in this area. [ X2000, 10 $\mu\text{m}$  bar, V = 5.6 km.s<sup>-1</sup>]*



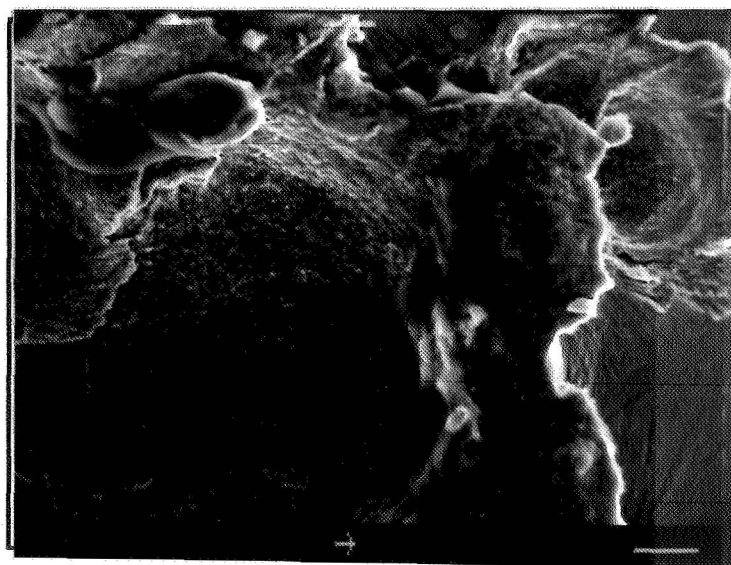
*Micrograph 7: Close-up of indentions on the trailing edge side of the crater shown in micrograph 4. The trailing edge crater lip can be seen in the lower portion of the micrograph. [X2000, 10  $\mu\text{m}$  bar,  $V = 5.6 \text{ km.s}^{-1}$ ]*



*Micrograph 8: 60 ° impact of a partially broken up particle. [X250, 100  $\mu\text{m}$  bar, Vel.= 4.6  $\text{km.s}^{-1}$ ]*



**Micrograph 9.** 60° impact caused by gun debris. The leading edge is to the far left, and the trailing edge is to the far right. [X250, 100  $\mu\text{m}$  bar, Vel.= 6.5 km.s<sup>-1</sup>]



**Micrograph 10.** Close-up of the crater shown in micrograph 9. Particle residue is located on the inside of the trailing edge of the crater lip (white, glowing material) and at the upper left-hand portion of the photograph. [X900, 10  $\mu\text{m}$  bar, Vel.= 6.5 km.s<sup>-1</sup>]